Aerodynamic Study of Superstructures of Megayachts

Eirini Trivyza[1*] and Evangelos Boulougouris[2]

1&2 Naval Architecture, Ocean and Marine Engineering,
University of Strathclyde, Glasgow, G4 0LZ, United Kingdom

Abstract: The paper provides an insight to the general flow characteristics around a yacht's superstructure, the air-wake felt by the helicopter at the helipad, with respect to the operational limits, and attempts the creation of a database of aerodynamic coefficients, for a range of incident flow angles. The flow is simulated using Star CCM+ solver, with a RANS k-ω SST model, for two different speeds and 5 different incident angles. The flow is observed to be highly rotational, turbulent and with large areas of flow separation. Furthermore, the flow characteristics are magnified as the incident angle increases. It is identified that geometric changes of the superstructure are required to improve the flow and the helicopter operations should be prohibited for the maximum speed, since they fail to comply with the existing regulatory framework. Finally, the human body resilience to wind intensity and turbulence must be introduced into the design process.
Keywords: Computational Fluid Dynamics (CFD); Yacht Aerodynamics; Ship Airwake; Helicopter Operation
Article ID: 1671-9433(2010)01-0000-00

1 Introduction

Since yachts were first introduced, they have represented a certain lifestyle and served as a symbol of status and social statement for their owners (Barnes, 2010). As a result, yacht design is dictated not only by performance, safety and comfort, as for the majority of vessels, but freedom, luxury and aesthetics are of great importance for the potential buyers (Francesetti, 2006). With respect to yacht performance, systematic studies of the ship hull, propeller, and appendages are undertaken. Moreover, when considering safety and comfort, the seakeeping behaviour and the levels of noise and vibration on board are examined. But freedom, luxury and aesthetics, even if they are non-technical terms and cannot be easily quantified, they must be translated as part of the design (Nuvolari, 2011). For these conditions to be satisfied, studies that are not traditional in mainstream naval architecture are undertaken. For example, the examination of the flow in the areas where the passengers spend most of their time or a study on the downwash of the exhaust plume, can give valuable information on the quality of the experience on board the vessel. Also, the positioning of the helipad can affect the aesthetics of the yacht and at the same time, the capability of the pilot to land the helicopter under any circumstances, will indicate if the luxurious needs of the owner, can be catered at all times (Harries and Vestings, 2010).

Aerodynamics is a subject which does not commonly affect the naval architects design decisions. However, for more than twenty years, significant studies have been conducted on the exhaust gas dissipation at the topsides of cruise ships, ferries and naval vessels and on how the air-wake created by the superstructure affects helicopter operations in naval vessels. This paper examines the aerodynamic behaviour of the superstructures of mega-yachts and the impact of the superstructure air-wake on the helipad, with the use of CFD.

2 Review of literature

Aerodynamic studies are not common for most ship types. Nevertheless, the complex problem of the airflow around the superstructure and the air-wake effects on the helideck, have been under the scope for naval vessels since 1974, due to the need to operate and perform their tasks under any given circumstances. Furthermore, many researchers have been involved with the creation of a database of aerodynamic coefficients of different ship types, which are used for the calculation of total resistance. The literature review for the two problems of interest was examined separately as follows.

2.1 Superstructure and air-wake

Smith and Mitchel in 1974, under the U.S. Navy Helicopter Compatibility Program, identified that design considerations should be made to minimise the unsteady phenomena created on the helipad, due to the superstructure geometry (Johns and Healey, 1989). Through a research on the airflow around the USN DD-963 Class Destroyer, the flow separation at the sharp edges was successfully captured and the importance of incident angle, with respect to the flow characteristics, was highlighted (Ibid.). In 1992 hot-wire anemometry tests were undertaken for incident angles of 0 to 90 degrees for the collection of data that would be used for helicopter flight simulations. It was noticed that the flow characteristics changed dramatically as the angle increased and the lowest and highest turbulence intensity levels were identified at 0

Received date:
Foundation item: Supported by University of Strathclyde
***Corresponding author Email: eirini.trivyza.2013@uni.strath.ac.uk**

and 90 degrees respectively (Rhoades and Healey, 1992). Under the scope of The Technical Cooperation Program, a generic Simple Frigate Shape (SFS) was examined for different wind angles with flow visualisation tests and the use of CFD, showing that the simulation results were in good agreement with the experimental ones (Wilkinson et al., 1999).

Tai and Carico (1995) used the solver CFL3D, which was based on a RANS code, to perform simulations on Healey's DD-963 model for a incident angle of 30 degrees for two different speeds. The results were very close to the experimental ones and it was noticed that the flow characteristics, due to separation, were only affected by the geometry of the edges and not the flow velocity. Reddy et al. and Polsky, using FLUENT and k-ε model for closure studied the SFS model and a LHA-Class ship respectively, producing results almost identical to the experimental ones (Padfield, 2007; Polsky, 2002). With the help of FLUENT solver and by using Detached Eddy Simulation (DES) with k-ω turbulence model and unstructured grid, Forrest and Owen (2010) performed simulations for the SFS and Type 23 for incident angles of 0, 10, 30, 45 and 90 degrees. The values obtained from their research were closer to the ones measured in sea trials than the experimental ones. Kaaria et al. (2013) measured the effect of the superstructure air-wake to the helipad for wind over deck angles of 30 and 45 degrees and introduced geometric modifications to minimise the effects of flow separation and vortex shedding.

Superstructure aerodynamics studies have mainly focused on naval vessels. Nevertheless, Frazer-Nash (2007) based on these approaches, addressed the issue of helicopter operations on Megayachts and highlighted that inadequate information is given in Large Yacht Code and CAP437, with respect to the required flow characteristics at the aft of the superstructure. Finally, Safety at Sea (2012) performed a series of simulations to examine the flow conditions at the outdoor spaces of the Oasis of the Seas. Based on these findings, shape optimisations were undertaken at the discovered problematic areas, leading up to 90% decrease of velocities at certain points.

2.2 Air Drag

Molland et al. (2011) performed a series of tests and identified that the air drag of the above waterline part of the vessel was a very small percentage of the total resistance varying from 2 to 6% depending on the vessel. The only case where it could significantly affect the total resistance was in beam winds for large vessels, such as containerships. These studies did not include yachts, however for passenger vessels, where the ratio between, above and below waterline area resembled that of yachts, the air drag was 6% of the total resistance.

With respect to aerodynamic drag coefficient (Cd) estimations, many researchers have published regression formulae available for the resistance calculation. The most commonly used were of Isherwood (1973), Van Berlekom (Kwon, 1981) and Blendreman (Schneekluth and Bertram, 1998). These are available in literature and suggested by ITTC for total resistance calculations (…).

Isherwood in 1972 performed data analysis for model tests of merchant ships and came up with a regression formula for the calculation of the drag coefficient for varying wind angles. This involved the use of tabulated constants, for varying wind angles, the lateral and transverse projected area above the waterline and dimensional characteristics of the vessel. The results of this method were recommended from ITTC for merchant ships. Nevertheless, it was not suggested for smaller vessels (Isherwood, 1973).

Van Berlekom in 1981 performed a series of wind tunnel model tests for tankers, containers, RO/ROs and some small crafts. The innovation introduced was that the ship's length squared was used as the reference area for the resistance estimation and the drag coefficient was a function of the projected area to the ship length (Kwon, 1981).

Most recently, Blenderman in 1996 undertook a number of tests for a great range of vessels and produced air drag coefficients for head (CdlAF) and beam winds (Cdl) (Schneekluth and Bertram, 1998). The results are illustrated in Figure 1.

	CD_t	CD_{lAF}
Car carrier	0.95	0.55
Cargo ship, container on deck, bridge aft	0.85	0.65/0.55
Containership, loaded	0.90	0.55
Destroyer	0.85	0.60
Diving support vessel	0.90	0.60
Drilling vessel	1.00	0.70–1.00
Ferry	0.90	0.45
Fishing vessel	0.95	0.70
LNG tanker	0.70	0.60
Offshore supply vessel	0.90	0.55
Passenger liner	0.90	0.40
Research vessel	0.85	0.55
Speed boat	0.90	0.55
Tanker, loaded	0.70	0.90
Tanker, in ballast	0.70	0.75
Tender	0.85	0.55

Figure 1 Blenderman coefficients for wind resistance

This paper extends the research that has been developed on superstructure aerodynamics to Megayachts aerodynamics, by examining a generic superstructure and identifying the main flow characteristics. This gives an insight on how the geometrical characteristics affect the flow at the outdoor spaces and in turn the passenger comfort and helicopter

operations. Furthermore, it attempts the creation of a database of aerodynamic coefficients for a range of incident angles, to complement the existing studies on the subject.

3 Computational details

Simulations were performed with the commercially available finite-volume code Star-CCM+® (CD-adapco, 2015), using RANS with SST k-ω turbulence model. The computations gave results for a scaled model of the yacht superstructure for two different speeds, the maximum and minimum one respectively, referred to as V1 and V2 and for incident angles of 0, 15, 30, 45 and 90 degrees. The two velocities reflected the real operational ones, of 5 and 20 knots, which are the conditions a yacht experiences moored and travelling with maximum forward speed.

3.1 Geometry and Mesh Generation

The geometry was based on a simplified superstructure of a yacht of 71.34 m Loa. This was created according to the construction drawings of an existing vessel and was modified to reflect general shape characteristics found in most yacht's above waterline body. To minimise the computational time and the size of the domain a scaled model was employed for the simulations. The scaling process followed geometric and dynamic similarity laws and from Reynolds similarity for viscous flows, velocities that represented the real ones were calculated.

Table 1 Model and Ship Characteristics

Loa of ship [m]	71.34
Loa of model [m]	14.27
V1 ship [m/s]	2.5
V1 model [m/s]	12.5
V2 ship [m/s]	10
V2 model [m/s]	50

Through an iterative process the domain dimensions were selected for the model of 14.27 m length. To avoid distortion of the results a rectangular domain of 100 m length, 34 m breadth and 10 m height was created. To maintain the size of the cells constrained close to the surface of interest a volumetric control was created inside the fluid area (Fig.2).

Figure 2 Fluid domain and Volumetric control

For the purposes of this study two types of mesh were available in Star CCM+. The polyhedral cells possessed 10 to 15 faces on average and required small number of cells to analyse the flow. However, the prism layer mesh was more refined and captured better the boundary layer characteristics and near wall conditions. In addition, it provided the freedom of manipulating the cell size and distribution close to the surface, while outside the volumetric control, the cells were freely adjusted as moving towards the boundaries. Thus, the prism layer meshing was selected and a domain of almost 3 million cells was generated for the simulation (Fig.3).

Figure 3 Surface and Centre Plane Mesh

3.2 Physics model and Solution

The flow was modelled as viscous, incompressible, turbulent and time-dependent. The incompressibility statement though had to be examined for the model simulation, due to the significantly high speeds calculated from the scaling process. The Mach number for both speeds was under 0.15 resulting to a simpler flow simulation.

The turbulence model selected was k-ω SST which provided results of high accuracy with respect to the prediction of flow separation near wall, while at the same time, gave sufficiently good free stream results. The build in Star CCM+ treatment of y+ value was employed, leading to the adaptive assignment of the non-dimensional wall distance with respect to the location the flow was examined (Fig.3).

For the time discretisation the single stage Implicit Euler backward differencing method was selected. This provided first order accuracy comparing to other implicit schemes, but was able to remain stable over large values of time steps, while significantly decreasing the computational time. The time step was set to 0.1 second intervals for a simulation time of 30 seconds, starting from 100 inner iterations and gradually dropping to 10 inner iterations as the solution became more stable.

3.3 Simulations and assumptions

For the undertaken computations certain assumptions were made that would not significantly affect the results. Since the scope of the research was to determine the general flow characteristic the only velocity considered was the free-stream one and not a forward speed and an apparent wind angle. Also, the model was stationary and no ship motions were accounted for during the simulations.

In addition, the atmospheric boundary layer, which would lead to smaller velocity gradients at the free- surface, was not introduced into the flow modelling. Finally, the free-surface was not modelled and was considered as a wall boundary condition. The remaining boundary conditions

were selected as in all aerodynamic studies, with free-stream velocity inlet, pressure outlet, non-slip condition on the model surface and symmetry for the side and top boundaries.
A series of simulations were undertaken, with the final 10 most promising used for the discussion of the results. These are listed below:

I. Model at 12.5 m/s corresponding to real velocity of 5 knots for incident angles of 0, 15, 30, 45 and 90 degrees.
II. Model at 50 m/s corresponding to real velocity of 20 knots for incident angles of 0, 15, 30, 45 and 90 degrees.

4 Results and discussion

The results have indicated that for the two velocities selected the general flow characteristics remained the same, with only the magnitude of the physical quantities examined varying. As a result, only the highest speed simulation's outcome is included in this paper, since the maximum values were observed in this case.

4.1 General flow characteristics

In 0 degrees incident angle the flow characteristics were symmetrical in relation to the centreline. Maximum pressures were observed at three different locations, at the higher edge of the bow deck-line, at the front of the upper deck and at the centroid of the antenna mast. At the main deck edge in the fore part, top and side edges of the upper and bridge deck adverse pressure gradient was noticed, leading to the creation of air-bubbles. At 15 degrees the bow deck line stagnation point was moved at the port of the bow and maximum pressures were observed at the starboard of the upper deck frontal area. The starboard maximum pressure was not expected at this location, but was caused due to the local flow characteristics at the forward top of the main deck, where large flow separation was noticed. In addition, the flow separation insisted at the same locations as in 0 degrees. When moving to 30 degrees an extensive high pressure zone was identified at the port of the bow. In 45 degrees the maximum pressures were located as before, but occupying a larger part of the port side. At 90 degrees incident angle, high pressures were indicated at the side of the vessel subjected to the free-stream (Fig.4). In general the magnitude of pressure reached the highest value for 90 degrees, followed by 0 degrees and for the remaining angles it remained almost constant.

0 degrees

15 degrees

30 degrees

45 degrees

90 degrees

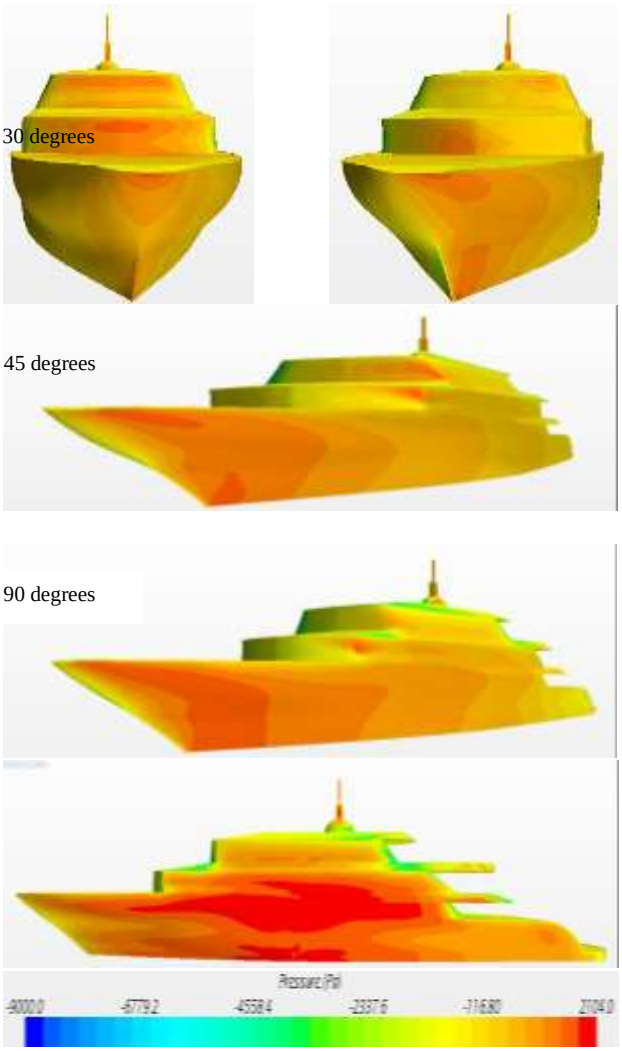

Figure 4 Pressure distribution for 0 to 45 and 90 degrees

Flow separation, recirculation areas and vortex shedding were the dominant characteristics for all incident angles. As it was noticed in the centreline planes plots of the velocity vectors, all the aforementioned insisted on specific areas for all incident angles. Nevertheless, there were variations of the intensity of the characteristics for different incident angles. The following plots provided a first insight on the flow behaviour at the centreline and generally problematic areas of the superstructure. Flow separation was noticed at the forward part of the main and upper deck and at the trailing edges of all the decks for the majority of the angles examined (Fig.5).

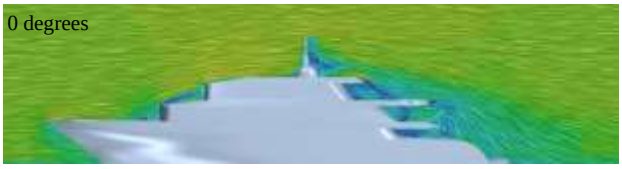

0 degrees

15 degrees

30 degrees

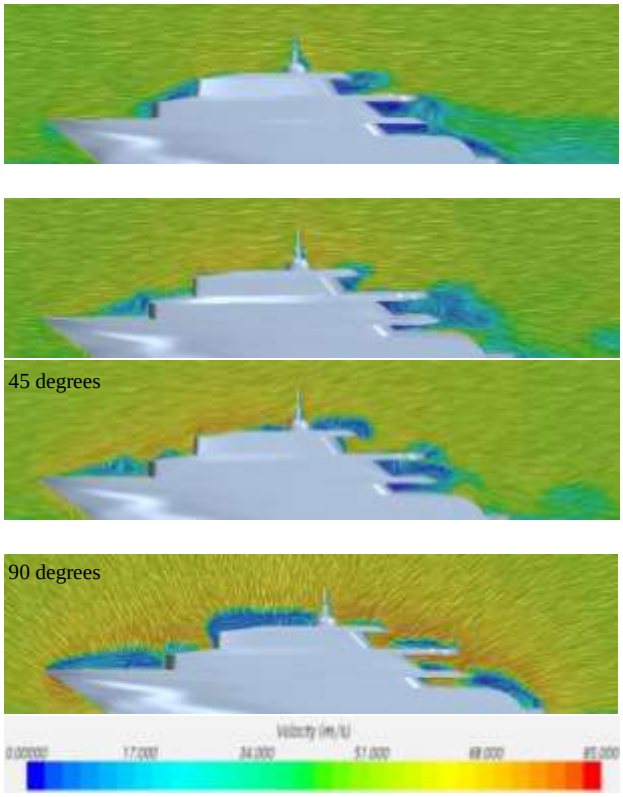

Figure 5 Velocity at centre-plane 0 to 45 and 90 degrees

For a more detailed analysis of the flow the streamline plots were employed. In 0 degrees significant flow recirculation was noticed at the top of the upper deck and between the main and upper deck at the forward part of the superstructure, due to the sudden geometry change. In addition, flow separation was noticed aft of the antenna must and low velocity recirculation zones for all decks aft of the superstructure. Due to 0 degree angle, two symmetrical around the centreline contra rotating vortices were created, with their main source located on the main deck. These were magnified by the contribution of eddies generated at the sharp edges of the remaining decks. Furthermore, two smaller vortical structures were created at the forward edges of the main deck, which died down at a very short distance from their generation point (Fig.6).

In 15 degrees the symmetry was lost and at the forward port side of the vessel, on the main and upper deck the flow was fully separated. On the other hand on the starboard side at the same locations the flow was attached. At the aft of the superstructure two main vortical structures were observed, one starting from the helideck trailing and side edges and the second one from the main deck. At a long distance from the vessel they were combined to one vortex (Fig.6).

For 30 degrees incident the flow was attached only at a relatively small part at the fore of the main deck at the starboard side and at the rest of this area the flow was separated leading to the creation of rotational behaviour. At the forward part of the main and bridge deck the first source of vortex generation was identified. Furthermore, the flow was detached from the surface at the starboard side edges and sides of the bridge and fly bridge giving rise to large eddies, which contributed to the rotational motion of the flow. All these characteristics, along with the contributions from the chaotic behaviour at the entire aft part of the superstructure caused the creation of a wide and stretched vortex (Fig.6).

In the case of the 45 degrees a main vortex was generated by the separation of the flow at the top of the main and upper deck at the forward part of the superstructure. The large eddies that were created from the side edges and sides of the bridge and fly bridge were sucked into the main vortical structure and contributed to its strength. Significantly chaotic and rotational behaviour of the flow was observed at the helideck and at the aft part of the main deck. At the end of the superstructure a wide and stretched vortex was noticed that slowly died down at a very long distance from the vessel (Fig.6).

Finally, for 90 degrees the flow was fully detached along almost all the surface of the model. Flow recirculation areas were the dominant characteristic and the speed reached the highest values noticed in all simulations. The body geometry and incident flow angle led to the generation of strong vortices at every top side of the decks which were combined to a stretched wide vortex at the starboard side of the vessel. These characteristics died down at a significantly long distance upstream. It was also derived that the 90 degrees angle gave the highest turbulence and vorticity levels, which were reflected by the completely chaotic behaviour behind the body (Fig.6).

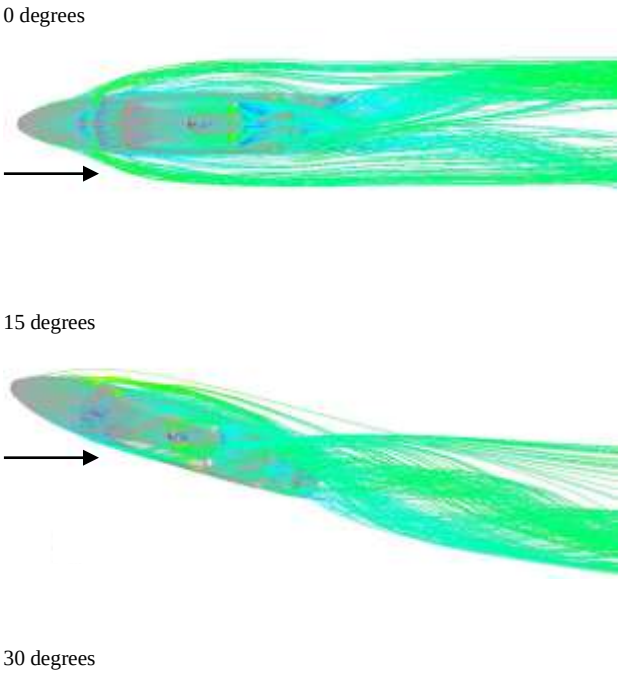

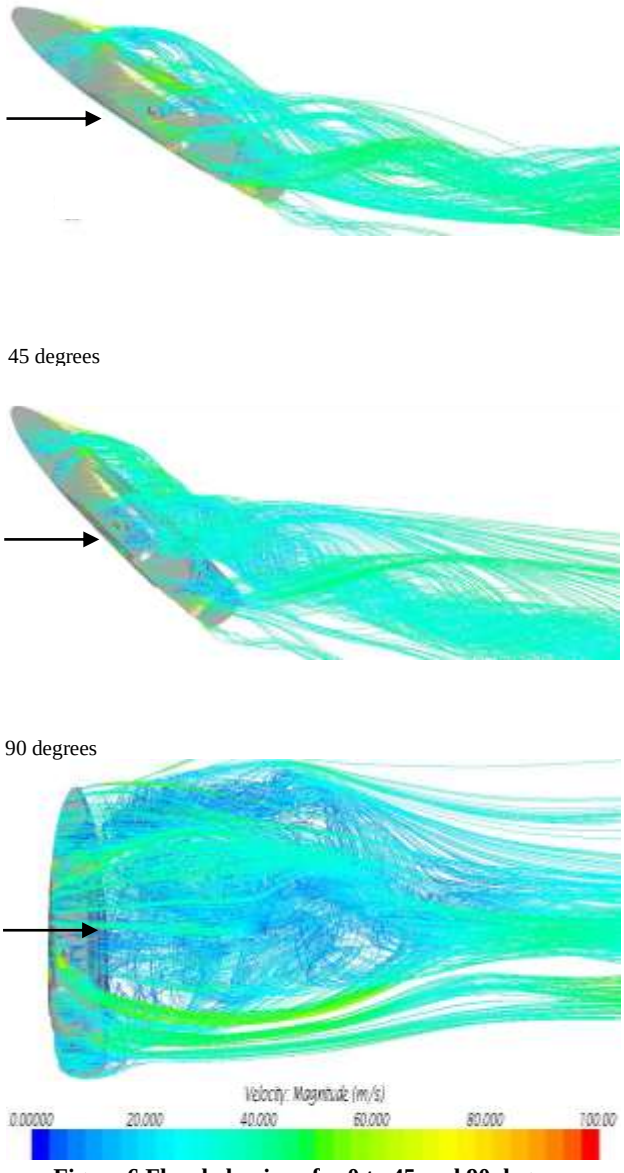

Figure 6 Flow behaviour for 0 to 45 and 90 degrees

4.2 Helicopter operations

Most yachts feature a helideck at the aft or fore of the superstructure. The aft location was used in this study, since it is the one most usually identified in vessels of this size. According to Large Yacht Code 3 (LYC3) and CAP437 the following criteria have been suggested for the wind conditions in the helipad:

I. The standard deviation [SDV] of the vertical airflow should be under 2.4 m/s.
II. The predicted rises of the temperature should not be 2 °C above ambient during a 3 second period at the location of the flight path.

The first condition was examined for both velocities selected, but the second one, which was strongly linked with the simulation of the exhaust gas from the funnel was not included as this would require a separate approach.

With respect to the lowest speed V1 it was noticed that regardless of the magnification of the chaotic behaviour at the aft of the superstructure with varying wind angles, the standard deviation of the vertical component of velocity was below the limiting value. For 0 degrees angle eddy motion was observed at the area, the flow was mostly separated at the bridge deck and was reattached at the centre of the landing area of the helicopter. Furthermore, for this angle symmetry of the flow was observed with respect to the centreline. As the angle increased, the flow remained attached at the majority of the port side of the helideck, but as moving to the starboard side the contribution of the smaller eddies created by the top, top edges and side edges of the fly bridge and bridge led to the creation of vortical structures at that side. When reaching 90 degrees large separation areas were noticed at the helideck location. Nevertheless, the SDV of the vertical flow was under the limit (Table 2).

On the other hand, when examining the results of the second velocity, which was significantly higher, the flow characteristics were magnified. The visual representation was the same as for V1, but the resulting values of turbulence intensity and local velocities were significantly higher. Once the results were collected and examined for all angles of interested it was realised the SDV of the vertical component of velocity was above the limit for all cases (Table2). The values calculated were almost twice the acceptable value with the highest one for 15 degrees angle. This led to the conclusion that for the vessels maximum speed the operation of the helicopter is significantly affected by the airwake of the superstructure and improvements are required. As a result, for V2 according to the rules the helicopter operations should be prohibited.

Table 2 Standard Deviation Criterion

Angles [deg.]	**0**	**15**	**30**	**45**	**90**
SDV_1 [m/s]	1.27	1.89	1.55	1.11	1.33
< 2.4 [m/s]	Ok	Ok	Ok	Ok	Ok
SDV_2 [m/s]	3.71	4.82	4.26	3.70	3.94
< 2.4 [m/s]	No	No	No	No	No

4.3 Aerodynamic Drag coefficient and Drag

The final part of this research was involved with the attempt of the creation of a database of validate aerodynamic coefficients. Since no wind tunnel tests were performed the results were compared with the ones introduced in the literature review and with road vehicle drag coefficients. This provided a first validation of the obtained coefficients and also, indicated the lack of substantial information on this subject, since most of the previous research has been developed mainly on merchant vessels.

For each one of the angles tested and for both velocities the drag coefficient was obtained, by employing the widely used drag equation and the transverse area projected to the freestream velocity plane. As expected the Cd was not affected by the speed changes, as it is a function of the body's geometry and specifically for aerodynamics, of the transverse projected area. The results for the two velocities were almost the same and an average of the obtained drag coefficients was used to indicate the variation of Cd with respect to the incident angle, as indicated in Table 3.

Angles [deg.]	Cd
0	0.327
15	0.439
30	0.667
45	0.773
60	0.827
75	0.868
90	0.940

Table 3 Drag coefficient for incident angles

Referring to the literature the most critical angles involving aerodynamic simulations were 0, 15, 30, 45 and 90 degrees, so a spline interpolation was used for the intermediate angles of 60 and 75 degrees (Table .3). The results for these angles (60 and 75 degrees) might not be as accurate as the ones that would have been obtained from an actual simulation, but they followed the trend of increasing drag coefficient with increasing angle. As a result, they could be used as a first good representation of the reality, for initial calculations.

In addition, from the derived results it was obvious that the incident angle played a critical role for the drag coefficient. Furthermore, it was noticed that for 0 degrees Cd was 0.327, which lies between 0.3 and 0.4 and it is the range of road vehicle drag coefficients. Also, it was very close to the passenger liner Cd of 0.4 given by Blenderman. Finally, for 90 degrees angle the Cd was 0.904, which was identical to Blendreman's for passenger liners and ferries.

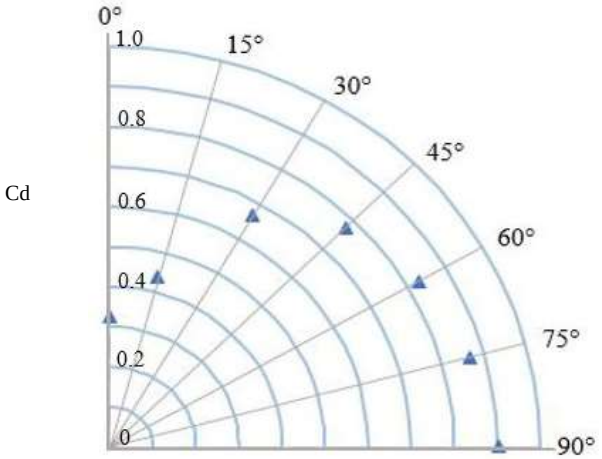

Figure 7 Polar plot of Cd variation

With respect to the total air drag the obtained values from the model were scaled to the ones found in the actual ship. It should be highlighted that the model actual forces did not vary a lot, since in the model very high velocities were used leading to high force values.

From the results it was obvious that the forces radically increased with the respect to velocity, which was expected since the resistance varies with the speed squared. Moreover, it was indicated that as the incident angle increased, the forces significantly increased as well (Fig.8, Fig.9). In addition, for both velocities the percentage of increased force was the same for increasing angle, leading to the conclusion that the rate of change of the force, with respect to the incident angle, was irrelevant of the velocity (Table 4). Although speed significantly affected the magnitude of the force, it was identified that in order to decrease the forces felt by the vessel in every velocity, the rate of force increase for increasing incident angles had to be minimised. Thus, the flow characteristics had to be improved for the examined angles.

Table 4 Drag and % difference between incident angles

Angle	Drag at V1 [N]	Drag at V2 [N]	% dif.
0	176.97	2831.55	-
15	289.05	4624.78	63.3
30	694.64	11114.22	140.3
45	1234.49	19751.92	77.7
90	2368.71	37899.31	91.9

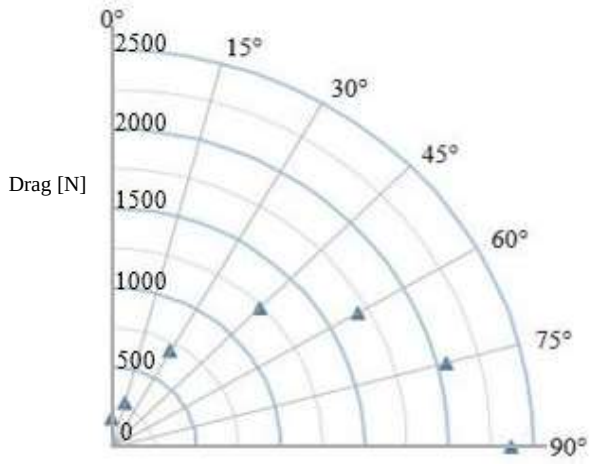

Figure 8 Air-drag for V1

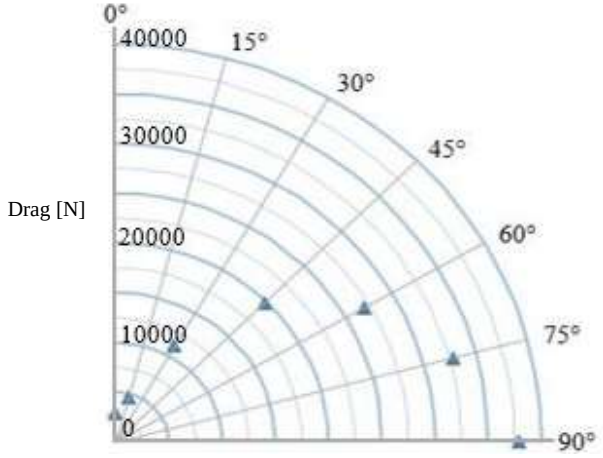

Figure 9 Air-drag for V2

5 Conclusions

During this research project the aerodynamic characteristics of a generic yacht superstructure were identified, for the most common minimum and maximum operating velocities and for incident angles of 0, 15, 30, 45 and 90 degrees. The following conclusions were derived:

I. For 0 degrees the maximum pressure was located at the frontal area of the upper deck and air bubbles were observed at the top of the main and upper deck. As the angle increased the highest pressure points moved at the port side and lower at the over waterline hull, close to the deckline edge. At 90 degrees the highest pressure values were identified at a zone of covering more than 2/3 of the side area located almost symmetrically about midships.

II. The flow at the aft of the superstructure was turbulent, highly rotational, with large shear areas and unsteady character, which was magnified as the incident angle increased. For 0 degrees the flow was symmetric about the centreline with two main contra rotating vortices generated by the flow separation on the main deck and eddies arising from the others decks trailing edges separation. As the angle changed the two vortices were reduced and combined to one wider and stretched vortex, found at the starboard of the vessel. In 15 degrees a strong vortex was created by the sides and helideck trailing edge separation and an equally strong one was created at the main deck, being combined to one, aft of the superstructure. After 30 degrees, the main source of vorticity was the large separation area at the fore part of the main deck and vortical structures created by the starboard sides and side edges were sucked into the main vortex. In 90 degrees the flow was erratic, chaotic and strongly turbulent at starboard side and fully detached at most surfaces of the vessel.

III. At the helideck area the flow was fully separated for 0 and 90 degrees. For the intermediate angles the flow was attached at the port side of the helideck and was separated as moving to starboard, beyond the centreline. For V1 the Standard Deviation of the vertical component of velocity was under the limits given by the rules. However, for V2 it was above the limit for all angles, indicating that helicopter operations for this angle should not be allowed.

IV. The air drag coefficient was the same for both velocities. The simulation results were in great agreement with existing data in marine studies and road vehicle aerodynamics and a first database of air drag coefficients for yachts was created.

V. It was identified that future work should be done on determining if generally applied geometry optimisations could improve the flow at the aft area of the superstructure. Also, a more consistent regulatory framework should by introduced for the helicopter operational limits in yachts. Finally, human susceptibility to wind speed and turbulent intensity should be introduced to future simulations.

Acknowledgement

The authors are grateful to the University of Strathclyde for its ongoing support. Results were obtained using the EPSRC funded ARCHIE-WeSt High Performance Computer (www.archie-west.ac.uk). EPSRC grant no. EP/K000586/1.. CD-adapco and Hellenic Bureau Veritas have also provided valuable assistance. The author would also like to thank the researchers of NAOME for their useful input on the software.

References

Barnes L (2010). *Luxury Yacht Interiors, 1870-192 as a Reflection of Gilded Age Social Status*, Ph.D. thesis, The Ohio State University, Ohio.

CD-adapco (2015). StarCCM+, www.cd-adapco.com.

Forrest J & Owen I (2010). An investigation of ship airwakes using Detached-Eddy Simulation. *Computers and Fluids*, **39**, 656-673.

Francesetti D (2006). Recreational Boat Yards: World Structure of the Industry and Importance of Social Responsibility. University of Pisa, Argostoli.

Frazer-Nash (2007). The military approach to superyacht comfort and safety. *Ship and Boat International*, **March/April**, 54-57.

Harries S & Vestings F (2010). Aerodynamic Optimisation of Superstructures and Components, COMPIT International Conference on Computer and IT Applications in the Maritime Industries, Gubbio, 335-347.

Isherwood R M (1937). Wind resistance of Merchant Ships. *RINA Supplementary papers*, **115**, 327-338

Johns K & Healey J (1989). The airwake of a DD-963 class destroyer. *Naval Engineering*, **101**, 36-42.

Kaaria C, Wang Y, White D & Owen I (2013). An experimental technique for evaluating the aerodynamic impact of ship superstructures on helicopter operations. *Ocean Engineering*, **61**, 97-108.

Kwon Y (1981). *The effect of weather, particularly short sea waves, on ship speed performance*. Ph.D. thesis, University of Newcastle upon Tyne, Newcastle.

Nuvolari C (2011). *The relationship between Customers, Marketing and Design Trends*. Royal Institution of Naval Architects, United Kingdom

Padfield G (2007). *Helicopter Flight Dynamics*. Wiley-Blackwell, Oxford, United Kingdom.

Polsky S (2002). Computational study of unsteady ship airwake. Reno: 40th Applied Aerospace Science Meeting and Exhibit.

Rhoades M & Healey J (1992). *Flight deck aerodynamics of a non-aviation ship*. Journal of Aircraft, **29**(4), 619-656

Safety at Sea (2012). CFD tools maximise open deck comfort. *Ship & Offshore*, **2**, 16-17.

Schneekluth H and Bertram V (1998). *Ship Design for Efficiency and Economy*. Butterwoth-Heinemman, Oxford, United Kingdom

Tai T (1998). Simulation and Analysis of LHD Ship Airwake by Navier-Stokes Method. Amsterdam: RTO - Fluid Dynamics Problems of Vehicles Operating Near or in the Air-Sea Interface.

Wilkinson C, Zan S, Gilbert N & Funk J (1999). Modelling and Simulation of Ship Airwakes for Helicopter Operations- A Collaborative Venture. Amsterdam: RTO - Fluid Dynamics Problems of Vehicles Operating Near or in the Air-Sea Interface.